COMPUTATIONS OF AIR FILMS AND PRESSURES BETWEEN WEBS AND ROLLERS FOR STEADY AND UNSTEADY OPERATING CONDITIONS

by

S. S. Kothari, K. Satheesh and F. W. Chambers
Oklahoma State University
USA

ABSTRACT

Numerical computations have been performed to predict the lubricating air film thickness and pressure for the entire region of smooth rotating support rollers wrapped by moving impermeable and permeable webs. Results have been obtained for both steady and unsteady web tensions for a range of operating parameters and web properties. The numerical predictions required the simultaneous solution of coupled partial differential equations. One equation is the dynamic motion equation for the finite length web and the other is the transient Reynolds lubrication equation for the air film. In these two-dimensional computations, the web is assumed perfectly flexible and infinitely wide, with negligible air escape at the edges. A finite difference formulation was developed for the two governing partial differential equations. Spacing and pressure between the moving web and the support roller were obtained as a function of both time and distance along the roller for cases of constant tension, step changes in tension, and sinusoidal fluctuations in tension. For constant tension, the transient solution converges to the steady state solution from approximate initial conditions. For the unsteady tension cases, computations are started from a steady state solution. The effects of the web velocity, tension, permeability, mass per unit area, roller velocity, radius, and slip flow on the air film thickness and pressure distribution were predicted.

NOMENCLATURE

b	web thickness
C	a constant
E	modulus of elasticity of web
h	air film thickness
h_o	constant central region (also initial) air film thickness
i	subscript indicating x-position along roller
I	moment of inertia of web cross-section

k	permeability coefficient of web
K	permeability of web
L	distance between the two end supports
L_1, L_2	location (x coordinates) of points on roller at which boundary conditions applied
m	web mass per unit area
n	superscript indicating time step
p	pressure
p_a	ambient pressure
p_0	initial pressure in air bearing region
R	roller radius
T	web tension
t	time
t^*	nondimensional time for step change in tension case
V	velocity
V_R	roller surface velocity
V_t	velocity of the air escaping through the permeable web
V_W	web velocity
w	half width of the web
x	spatial coordinate along the direction of web velocity
y	spatial coordinate along radial direction i.e. along web displacement
α	angle between web and horizontal reference line far from roller
$\delta(x)$	function describing roller surface geometry
ϕ	phase angle for oscillating tension case
λ	mean free path length
λ_a	mean free path length at atmospheric pressure
μ	dynamic viscosity of air
ν	kinematic viscosity of air
ρ_a	density of air

INTRODUCTION

Background

A web is defined as a material manufactured in continuous strip form, and efficient processing demands high speed transport over guide and drive rollers. This motion is accompanied by the development of an air film between the web and roller. This air film can function as a self-acting air bearing, supporting the web and preventing excessive abrasion, but allowing sufficient asperity contact to maintain traction. When the air film becomes too thick, traction for web drive and lateral position control is lost and excess air is wound into winding rolls, leading to undesired roll mechanical properties and defects. When the air film is too thin, abrasive surface damage can occur. Daly [1] reviewed the important variables affecting the traction between webs and rollers, identifying web speed, web tension, web permeability, and roll diameter as important. Knox and Sweeney [2] noted that the web roller air film problem matched the configuration of the self-acting foil bearing. The foil bearing already had been studied by tribologists with particular attention devoted to applications to magnetic tape recorder heads.

Self-Acting Foil Bearings

A schematic illustration of a self-acting foil bearing is presented in Figure 1. Foil bearings function as a result of the pressure developed in the air film between the foil (web) and shaft (roller) supporting the flexible foil against the forces of the tension, which are pulling the foil toward the shaft. Air is drawn between the foil and shaft through the action of viscosity dragging the air with the moving surfaces. No pressurized supply of air is used in self-acting bearings. The two surfaces, the foil and the shaft, may both be moving, or one may be stationary. Blok and van Rossum [3] introduced the concept of the foil bearing and performed the first foil bearing experiments and analysis. The analytical solution involves the coupled solution of the governing equations for the dynamics of the foil and the dynamics of the viscous air flow. Among the first derivations and solutions to simplified versions of these equations were those of Baumeister [4], Barlow [5,6] and Eshel and Elrod [7]. Gross [8] presents a concise survey of the earlier work on foil bearings with a derivation of the governing equations.

For most practical wrap angles, the solutions display three distinct regions. In the entrance region, as illustrated in Figure 1, the air film thickness smoothly decreases, while the pressure increases to the film pressure, p. In the central region, the air film thickness, h_o, and pressure, p, remain constant. In the exit region, the air film thickness increases from h_o to infinity, displaying a characteristic dip that the Reynolds equation shows is needed to accommodate a change in pressure gradient.

If simplifying assumptions are made, an equation may be derived for the air film thickness in the central, constant thickness region. Assuming incompressible flow for an infinitely wide impermeable web with perfect flexibility, the non-dimensionalized air film height in the central region is given by the following equation:

$$\frac{h_o}{R} = C\left(\frac{6\mu V}{T}\right)^{2/3} \tag{1}$$

Popularly, the constant C = 0.643, but different researchers have proposed slightly different values. See Ma [9] for different values and comparisons to measured film heights. Knox and Sweeney [2] proposed a change in Eq. 1 for application to web handling. They showed that for a system in which both the foil and the surface are in motion the equation becomes:

$$\frac{h_o}{R} = 0.643\left[\frac{12\mu V_W}{T}\right]^{2/3} \tag{2}$$

It may readily be shown that the two velocities are additive; V in Equation 1 is the sum of V_W and V_R, 6V becomes 12 V_W.= $6(V_W + V_R)$ when $V_W = V_R$. More sophisticated analyses are needed to incorporate more complex geometries and conditions that do not meet these simplifying assumptions.

Much of the literature on foil bearings has been concerned with applications to magnetic tape recorder heads. Eshel and Elrod [7] first presented accurate numerical solutions for the film thickness in the entrance and exit regions. Other works have incorporated the effects of compressibility, the bending stiffness of the tape, slip flow for very small film thicknesses, non-negligible fluid inertia, more complex geometries, and

external pressurization [6, 10-17]. Fully three-dimensional computations have been performed using both finite difference and finite element approaches [18,19]. Unsteadiness in foil bearing problems has been considered by a number of researchers, including, Eshel and Wildmann [20], Eshel [21], and Stahl, et al. [22].

A variety of numerical techniques have been used to solve foil bearing problems. Stahl, et al. [22] showed that a steady state foil bearing solution could be calculated faster by solving the transient problem from initial conditions to steady state rather than by direct coupling through a standard relaxation technique. Granzow [23] and Granzow and Lebeck [24] describe use of a Crank-Nicholson form of the finite difference equations for the time derivative terms allowing larger time steps. Tanaka, et al. [25] used an influence coefficient method for the tape equation and the Newton-Raphson iterative method for the Reynolds equation. Heinrich and Wadhwa [17] employed the Newmark finite element algorithm in their solution. Rongen [18] presented a finite difference solution for the three-dimensional foil bearing problem. Heinrich and Connolly [19] describe a three-dimensional finite element analysis of a self-acting foil bearing for recording head geometries.

All of these studies were performed for impermeable webs. For paper webs or other permeable webs, corrections in the Reynolds lubrication equation are suggested by the relationship given by Yamauchi, et al. [26] for the velocity of air leaking through permeable webs. The indicate that the air leakage through the web is proportional to the pressure difference across it, with a constant of proportionality that is the permeability coefficient of the porous medium. Brundertt and Baines [27] present measurements of air flow through paper sheets as functions of pressure difference at room temperature. Riddiford [28] studied the air entrainment phenomenon between a permeable paper web and a dryer surface, showing that the gap may be decreased by the entrained air passing through the paper and flowing out at the edges. He developed a mathematical model and solved to show the conditions under which axial variation in air film thickness can exist. Theoretical and experimental analysis of air films for the case of a permeable web by Watanabe and Sueoka [29] indicated a linearly decreasing, rather than a constant, central region air film thickness. The entrance and exit regions appeared to exhibit approximately the same behavior for both cases. Ducotey and Good [30] also performed experiments with permeable webs, with results displaying the linear decrease. They present an approximate predictive equation for the decrease in air film thickness in the central region.

APPROACH

Problem Formulation

To obtain solutions for these problems, a numerical technique was formulated to predict the air-film thickness and pressure between the moving web and the roller surface as functions of time starting from prescribed initial conditions and developing to either a steady state or steady state oscillations. This was done for the two dimensional case, an infinitely wide bearing, with constant cross-web air film thickness and pressure. The effects of web permeability are incorporated in the formulation.

To predict the lubricating air film thickness between the web and roller requires the simultaneous solution of coupled equations: one, the equation of motion for a finite length of the web and second, the transient lubrication equation for the air film. The

partial differential equations governing both the hydrodynamic lubrication and the web motion are described here. Almost all web handling applications involve an air film thickness which is much smaller than the radius of curvature of the lubricating film, allowing use of a Cartesian coordinate system.

Reynolds Lubrication Equation. The hydrodynamic lubrication equation, or Reynolds lubrication equation, represents a dynamic equilibrium of forces due to fluid pressure and viscous stresses in combination with conservation of mass. The form of the equation employed for this study is the following:

$$\frac{\partial}{\partial x}\left(h^3 p \frac{\partial p}{\partial x}\right) + 6\lambda_a p_a \frac{\partial}{\partial x}\left(h^2 \frac{\partial p}{\partial x}\right) = 6\mu(V_R + V_W)\frac{\partial}{\partial x}(ph) + 12\mu \frac{\partial}{\partial t}(ph) + 12\mu K p(p - p_a) \quad (3)$$

For this lubrication equation, fluid inertia and the variation of pressure across the thickness of the thin film are assumed negligible. This version of the equation further assumes that the lubricating fluid is an isothermal ideal gas with constant viscosity. The equation accounts for motion by both the web and the roller through the separate velocities, V_W and V_R. Slip flow effects, which are important for very small film thicknesses, are accounted for by the second term, with λ_a, the molecular mean free path at ambient conditions, following Granzow [23] and Granzow and Lebeck [24]. Fluid compressibility effects are accounted for by the derivatives of the (ph) product. The effect of the flow through the permeable web is given by the last term. The flow through the web is proportional to the local pressure difference across the web, with the through-flow velocity $V_t = K(p\text{-}p_a)$, as suggested by Yamauchi et al. [26]. "K" is the permeability of the web, with units of $(m^3/s)/(m^2\text{-}Pa)$.

Foil Equation of Motion. The foil equation of motion is a representation of Newton's second law for the foil or web in the direction normal to the direction of web travel. It is assumed that the deflection of the web is very small compared to the dimension of the support roller. The general equation is the following:

$$\rho b\left(\frac{\partial^2 y}{\partial t^2} + 2V_W \frac{\partial^2 y}{\partial x \partial t} + V_W{}^2 \frac{\partial^2 y}{\partial x^2}\right) + \frac{EI}{w}\frac{\partial^4 y}{\partial t^4} - \frac{T}{w}\frac{\partial^2 y}{\partial x^2} = p - p_a \quad (4)$$

If we consider the web as a plate in tension, an order of magnitude analysis indicates that the bending stiffness term is very small compared to the tension term for many webs. Then, neglecting this term, the equation becomes the equation for a web with zero stiffness, a perfectly flexible web:

$$\rho b\left(\frac{\partial^2 y}{\partial t^2} + 2V_W \frac{\partial^2 y}{\partial x \partial t} + V_W{}^2 \frac{\partial^2 y}{\partial x^2}\right) - \frac{T}{w}\frac{\partial^2 y}{\partial x^2} = p - p_a \quad (5)$$

This is the form of the equation used in this study.

Geometric Configuration, Initial Conditions and Boundary Conditions. The geometric configuration used in the computations is illustrated below in Figure 2. A finite length of web moves at constant velocity, V_W, over a roller located between two other support rollers. Deflection of the web away from its equilibrium position is denoted by y(x,t) and the air film thickness between the roller and web is denoted by h(x,t). Following the approach of Granzow [23] and Granzow and Lebeck [24], a

function $\delta(x)$ is used to describe the roller surface geometry in terms of distance from the reference line shown in Figure 2. Also using their approach, boundary conditions are applied as the free spans of the web approach the roller, points L_1 and L_2, rather than at great distances from the roller. These points are significantly outside the points at which the web run is approximately tangent to the roller. Computations then are performed only within these points. Granzow and Lebeck showed that this is an accurate and efficient means of solving foil bearing problems.

The film thickness, h, and the foil displacement, y, are related through the following equation:

$$h(x,t) = y(x,t) - \delta(x) \tag{6}$$

Boundary conditions are applied at the points, L_1 and L_2, within which the tangency points occur. The boundary conditions amount to clamped ends. The boundary conditions specify the displacement, y, and the slope of the displacement, $\partial y/\partial x$, or y_x:

$$\begin{aligned} y(L_1,t) &= y(L_1,0) = \text{constant} \\ y(L_2,t) &= y(L_2,0) = \text{constant} \\ y_x(L_1,t) &= y_x(L_1,0) = \text{constant} \\ y_x(L_2,t) &= y_x(L_2,0) = \text{constant} \\ p(L_1,t) &= p(L_2,t) = p_a \end{aligned} \tag{7}$$

For the steady state calculations, for the domain within the tangency points, the initial conditions for air film thickness and the pressure are taken as the values that may be calculated for the constant thickness region:

$$h = h_o = 0.643R\left(6\mu\frac{(V_R + V_W)}{T}\right)^{2/3} = \text{constant} \tag{8}$$

$$p = p_o = p_a + \frac{T}{R} = \text{constant} \tag{9}$$

For the region outside the tangency points the displacement is taken to be linear and the pressure to be atmospheric. The coordinates of the two tangent points are calculated directly from the geometry, using the length, the roller radius, and the web angle:

$$\begin{aligned} x_o &= 0.5L - (R + h_o)\sin\alpha \\ y_o &= (\delta_{max} - R) + (R + h_o)\cos\alpha \end{aligned} \tag{10}$$

For the step change in tension and sinusoidal tension fluctuation cases, the program was started and allowed to reach the steady state solution from these initial conditions before the transient tension was applied.

Numerical Formulation and Solution Technique

The numerical solution to the governing equations is accomplished through a finite difference formulation. The two governing equations, Equations 3 and 5, are coupled through the pressure and Equation 6, which links the web displacement and the lubricating air film thickness. The equations are converted to finite difference form and

solved simultaneously using the boundary conditions and initial conditions described earlier. The solutions start from the initial conditions and step forward through time, providing transient and finally the steady state results.

The coupling of the equations is accomplished by first, at a given time step, solving the finite difference form of the lubrication equation for the pressure, p(x,t), using the existing solution (for the first step, the initial conditions) for the air film thickness, h(x,t). Then the finite difference form of the web equation of motion is used with the newly computed values of the pressure to compute new values of the web displacement, y(x,t). This procedure is performed iteratively until steady state is reached.

After converting to finite difference form, the equation of motion for the web reduces to the form:

$$\mathbf{B}_1 y_{i-1}^{n+1} + \mathbf{D}_1 y_i^{n+1} + \mathbf{A}_1 y_{i+1}^{n+1} = \mathbf{E}_1 \tag{11}$$

where, $\mathbf{B}_1$, $\mathbf{D}_1$, and $\mathbf{A}_1$ are constants containing coefficients from Equation 5 and $\mathbf{E}_1$ contains the values of foil displacement, y(x,t) at time step **n** and (**n-1**) and, pressure, p at time step **n**. Similarly the finite difference form of the lubrication equation is the following:

$$\mathbf{B}_2 p_{i-1}^{n+1} + \mathbf{D}_2 p_i^{n+1} + \mathbf{A}_2 p_{i+1}^{n+1} = \mathbf{E}_2 \tag{12}$$

where, $\mathbf{B}_2$, $\mathbf{D}_2$, $\mathbf{A}_2$, and $\mathbf{E}_2$ contain the values of pressure, p, at time step, **n**, and values of air film gap, h(x,t), at time step, **n**, and (**n+1**) obtained solving Equation 11. The nonlinear finite difference form of the Reynolds Lubrication equation is linearized using the approach of Stahl, et al. [22] with an approximation at the old time step **n** instead of the new time step (**n+1**) in those terms involving products of p and its derivatives. For more details, see Kothari [31].

The finite difference forms of the governing equations reduce to tri-diagonal matrices (a benefit of assuming perfect flexibility for the web), and solutions are obtained using the Tri-Diagonal Matrix Algorithm. This applies the Gauss elimination method as described by Lilley [32]. The solution grids of mesh size Δx and time steps Δt are chosen with Δt limited to maintain numerical stability. A mesh of 125 points in the x direction covering the distance between the points L_1 and L_2 was found adequate and used for all calculations. For the parameters studied, time steps of 5 μs or smaller were necessary to maintain numerical stability.

Convergence criteria for the steady state computations were applied to the air film thickness. Convergence was judged to occur when the sum of the 125 nondimensional changes in air film thickness between iterations was less than 10^{-4}. The same convergence criterion was applied for the two sides of the step increase case. For the sinusoidal tension fluctuation case, the same magnitude criterion was applied, but the comparisons were made for points 2π apart in angle; iterations at the same phase point in the steady state oscillation cycle.

RESULTS AND DISCUSSION

Results are presented in this section for computed air film thicknesses for steady state cases with steady, constant tension and for transient cases with step increases in tension and sinusoidal oscillations in tension. For all of the results presented, the non-

dimensional distance coordinate in the figures corresponds to $(x-L_1)/(L_2-L_1)$. Thus 0.0 corresponds to $x = L_1$, the upstream point at which boundary conditions are applied, and 1.0 corresponds to $x = L_2$, the downstream point at which boundary conditions are applied. The tangency points used in the initial conditions lie between L_1 and L_2.

Results for Constant Tension

Computations were performed with steady constant tension for a variety of operating parameters. Initial computations were performed to allow comparison and code validation with results in the magnetic recording tape literature for a web (magnetic tape) moving over a stationary cylinder (recording head). A 40 mm diameter roller was used for this case with tension, $T = 277$ N/m and web velocity, $V_W = 2.54$ m/s. The angle of wrap was approximately 20 degrees. The transient air film thickness development from initial conditions to steady state is shown in Figure 3. Steady state is reached in approximately 6 ms. The steady state time depends upon the wrap angle and the combined speed of the web and roller surface. The points of tangency are recognizable as the corners in the initial condition profile. These steady state results yield air film thicknesses in the central region that are within 4% of the results given by Stahl, et al. [22] and within 5% of the value predicted by Equation 2. The shapes of the profiles also agree well with results in the literature. These comparisons were judged to validate the computational approach. The transient pressure profiles display smaller transient oscillations than the film thickness.

Incorporating the effects of slip flow tends to reduce the air film thickness, with the effect decreasing at higher web velocities. This effect is expected, for high speed web handling applications have higher air film thicknesses, which are very large compared to the 10^{-8} m mean free path of air. Thus neglecting slip flow effects is a good approximation for many web handling applications.

Results for Impermeable Webs with Constant Tension. After validations against magnetic recording literature results, computations were performed for web handling configurations with both the web and the support cylinder moving. A roller radius of 20 cm was used for computations with tensions varying from 88 to 262 N/m and velocities varying from 5.1 to 15.2 m/s. For this roller, $L = 0.85$ m, $L_1 = 0.35$ m, and $L_2 = 0.50$ m. The tangency points corresponded to $x = 0.390$ m and 0.453 m, corresponding to nondimensional positions of 0.2893 and 0.7107. The magnitudes of the computed air film thicknesses in the central region showed the trends expected from Equation 2 with increasing tension reducing and increasing velocity increasing the air film thickness. It was also observed that the length of the central constant gap region increases with increasing tension or decreasing velocity. Likewise, the amplitude of the dip in the exit region scaled with the central region air film thickness increases noticeably with increasing tension and decreasing velocity. The period for the transient computations to reach steady state also exhibited decreases as the velocity of the web increased, other parameters remaining the same.

The effect of web mass per unit area on the steady state air film thickness profiles also was investigated. A tension of 263 N/m was used with velocities of 5.1 m/s and 15.2 m/s with web mass varying from 0.02 to 0.1 kg/m^2. For the lower velocity, the air film profiles for different web mass virtually coincide, with less than a 1% change in central region film thickness for nearly a 400% increase in web mass. The results for the higher velocity case are shown in Figure 4. For this case the increase in steady state air

film thickness is about 11.5% in the central region for the same increase in web mass, showing that the effects of mass increase significantly with velocity. The exit region dip seems to show effects very similar to those that can be observed in the central region. Thus for the same velocity, a heavier web should have a slightly larger film thickness, which might have implications for web traction.

Results for Permeable Webs with Constant Tension. Results are presented here for computations that include the effects of web permeability. As shown previously, the effect of web permeability may be modeled as a flow through the web that is proportional to the difference between the film pressure beneath the web and the surrounding ambient pressure. Watanabe and Sueoka [29] have presented experimental measurements of air film thicknesses for permeable webs along with a limited description of an analytical treatment of the problem. Ducotey and Good [32] present measurements along with an approximate equation for the prediction of the film thickness. Both works show that the film thickness in the central region exhibits a nearly linear decrease as air flows out through the web. Ducotey and Good's equation predicts the linear decrease as follows:

$$h = 0.643R\left[\frac{6\mu(V_R + V_W)}{T}\right]^{2/3} - 2\left[\frac{KT}{(V_R + V_W)}\right]\theta \qquad (13)$$

Here, θ is the spatial coordinate along the surface in radians and K is the web permeability. This equation is based on the assumption that the air flow through the web and the film pressure remain constant and independent of θ. The computations presented here were performed for a roller radius of 30.48 cm to allow comparisons with the results of Ducotey and Good. For this roller, L = 1.26 m, L_1 = 0.520 m, and L_2 = 0.7455 m. The tangency points corresponded to x = 0.585 m and 0.679 m, corresponding to nondimensional positions of 0.2902 and 0.7098. .Figure 5 compares the air film profiles for impermeable and permeable webs running at a web velocity, V_W = 15.2 m/s, and tension, T = 124 N/m. For the permeable case, one may observe the characteristic, nearly linear decrease in the air film thickness as well as a decrease in the magnitude of the exit region dip, although the minimum film thickness is smaller. Ducotey and Good observed that web touch downs are possible in the exit region for permeable webs. Figure 6 displays the effects of web and roller velocity on air film thickness profiles for the web permeability K = 0.3 x 10^{-5} (m^3/s)/(m^2-Pa) for conditions of constant tension, T = 124 N/m. The results display nearly linear decreases in air film thickness for the central region, and entrance and exit region behaviors similar to those of impermeable webs.

The decrease in the air film gap for the central region is a function of web-roller velocity, web tension and web permeability. The decrease is not precisely linear, for the flow rate through the web varies with the film pressure, which must change as the air film thickness and radius of curvature of the web decrease. Figure 7 displays the results of computations for conditions matching those of Ducotey and Good [32], T = 88 N/m, V_W = 15.2 m/s, and K = 0.52 x 10^{-5} (m^3/s)/(m^2-Pa). It may be observed that the computed decrease is not precisely linear, but that Equation 13 provides a very good approximation to the decrease for typical web handling parameters and web permeability. This behavior also was observed in computations for other parameters.

Results for Unsteady Tension

The transient computation capabilities of the technique, already displayed in the steady state results, also were used to examine web response to transients in the applied tension. The response of webs to tension transients is of interest because of possible oscillations that may result in the web making damaging contact with the roller. Cases of step increases in tension and sinusoidal oscillations in tension were examined for both impermeable and permeable webs.

Step Increases in Tension. The computations for step increases in tension were performed by starting the computations at the approximate initial conditions used for the steady state studies, letting the solution converge to the steady state value for the low tension condition, and then applying the step increase in tension, running the code until the solution converged to steady state for the increased tension. The air film profiles at various times in the response to the step increase in tension are presented for a 50% step increase in tension from an initial tension, T = 175.334 N/m, at a web velocity, V_W = 10.16 m/s, for a web with a mass of 0.0922 kg/m^2 in Figure 8. The times in the figure are nondimensionalized with $t^* = (tV_W)/(2\pi R)$. Thus for a value of $t^* = 1$, the time would equal the time for one revolution of the roller.

One may observe that for these conditions the profiles do display something of a traveling wave response with little evidence of overshoot that could result in damaging contact between the web and roller. Figure 9 displays results for a case that is identical except that the web is permeable, with permeability, K = 0.052 E^{-5} (m^3/s)/(m^2-Pa). The behavior is similar to that of the impermeable web, but the response appears to be slightly more rapid. It may be reasoned that the decrease in film thickness is aided by the escape of air through the web.

Sinusoidal Tension Oscillations. The computations for sinusoidal oscillations in tension were performed by starting the computations at the approximate initial conditions used for the steady state studies, letting the solution converge to the steady state value for the mean tension, and then applying the sinusoidal oscillations in tension, running the code until the solution reached steady state oscillating conditions. Convergence to steady state oscillations was checked by evaluating the differences in the air film thickness profiles from one cycle to the next. The mean tension was 175.334 N/m, the same as the initial tension for the step increase cases. All other parameters also were the same as those of the step increase case. The amplitude of the tension fluctuation was 50% of the mean tension.

The frequency of the tension oscillation for the results presented was set to a value corresponding to twice an expected natural frequency for a web span of L/2. The natural frequency equation used was the following:

$$f = \left(\frac{1}{2L}\right)\left(\frac{T}{m + \rho_a \pi w / 4}\right)^{1/2} \tag{14}$$

Results for these oscillating tensions are shown in Figure 10 for an impermeable web and in Figure 11 for a web with permeability K = 0.052 E^{-5} (m^3/s)/(m^2-Pa), as used for the step increase computations. The results shown are identified with a phase angle ϕ representing the position in the cycle of oscillations.

While the results presented do not include a complete and uniform distribution of points in the cycle, they do present a good view of the web response to sinusoidally oscillating tension. For this case of large amplitude tension fluctuations, the web response also is rather large. It is evident that the nonlinear steady state dependence of the air film thickness on the tension is reflected in this dynamic response as well. It appears that somewhat larger amplitude movement of the web occurs at positions above the steady state film thickness than below.

Summary

The development of a computational method to predict the time-dependent air film thickness distribution and film pressure between an infinitely wide, smooth, perfectly flexible web and a smooth roller has been presented. The web may be either permeable or impermeable. The method accounts for the mass of the web, the compressibility of the air and slip flow effects. Results of computations using the method have been presented for steady and unsteady cases of impermeable and permeable webs.

CONCLUSIONS

The following conclusions may be drawn from the results of this study based upon the range of web parameters considered.

1.) A relatively simple program has been developed to predict time-dependent air film thicknesses and film pressures for infinitely wide, perfectly flexible, smooth webs moving over smooth rollers. The results obtained display good agreement with results for cases in the literature. The results obtained from the program effectively show the influence of a number of web handling parameters.

2.) The length of the central constant air film thickness region increases with increasing tension or decreasing velocity.

3.) The effects of web mass per unit area are small at low velocities, but increased mass results in somewhat thicker air films as web velocities increase.

4.) Slip flow effects are very small and become insignificant as web speeds and film thicknesses increase.

5.) Permeable webs display nearly linear reductions in central region air film thickness with distance along the roller. These effects depend upon web tension and velocity. The minimum air gap at the exit region for these webs is less than for impermeable webs.

6.) The transient response of web air films to step increases in tension displays traveling wave-like characteristics and is not predicted to result in roller contact for the conditions studied. Permeable webs display slightly faster response than impermeable webs.

7.) The response of air films to sinusoidal oscillations in tension is nonlinear with larger amplitude fluctuations above the location of the web at mean tension conditions.

ACKNOWLEDGMENTS

The authors gratefully acknowledge the support of the Oklahoma State University Web Handling Research Center and its member companies as well as the advice of Dr.

Alan O. Lebeck, Mechanical Seal Technology, Albuquerque, New Mexico, which was instrumental in establishing the approach for the computations.

REFERENCES

1. Daly, D.A., "Factors Controlling Traction Between Webs and Their Carrying Rolls," TAPPI Journal, pp. 88A-90A, Vol. 48, September, 1965.
2. Knox, K.L., and Sweeney, T.L., "Fluid Effects Associated With Web Handling," Ind. Eng. Chem. Process. Design. Dev., Vol. 10, pp. 201-205, 1971.
3. Blok, H., and van Rossum, J.J., "The Foil Bearing - A New Departure In Hydrodynamic Lubrication," Lubrication Engineering, Vol. 9, No. 6, 1953, pp. 316-320.
4. Baumeister, H.K., "Nominal Clearance of the Foil Bearing," IBM Journal of Research and Development, Vol. 7, pp. 153-154, 1963.
5. Barlow, E.J., "Derivation of Governing Equations for Self-Acting Foil Bearings," Trans. of ASME, Journal of Lubrication Technology, Vol. 89, pp. 334-340, 1967.
6. Barlow, E.J., "Self-Acting Foil Bearings of Infinite Width," Trans. of ASME, Journal of Lubrication Technology, Vol. 89, pp. 341-345, 1967.
7. Eshel, A., and Elrod, H.G., Jr., "The Theory of the Infinitely Wide, Perfectly Flexible, Self-Acting Foil Bearing," ASME Journal of Basic Engineering, Vol. 87, No. 4, pp. 831-836, 1965.
8. Gross, W.A., Matsch, L.A., Castelli, V., Eshel, A., Vohr, J.H., and Wildmann, M., Fluid Film Lubrication, John Wiley & Sons, Inc., NY, 1980.
9. Ma, J.T.S., "An Investigation of Self-Acting Foil Bearings," Trans. of ASME, Journal of Basic Engineering, Vol. 87, pp. 837-846, 1965.
10. Eshel, A., "Compressibility Effects on the Infinitely Wide, Perfectly Flexible Foil Bearing," ASME Journal of Lubrication Technology, Vol. 90, pp. 221-225, 1968.
11. Eshel, A., "On Controlling the Film Thickness in Self-Acting Foil Bearings," ASME Journal of Lubrication Technology, Vol. 92, pp. 359-362, 1970.
12. Eshel, A., "On Fluid Inertia Effects in Infinitely Wide Foil Bearings," ASME Journal of Lubrication Technology, Vol. 92, pp. 490-494, 1970.
13. Eshel, A., and Lowe, A.R., "Experimental and Theoretical Investigation of Head to Tape Separation in Magnetic Recording," IEEE Trans. on Magnetics, Vol. MAG-9, No. 4, pp. 683-688, 1973.
14. Eshel, A., "Reduction of Air Films in Magnetic Recording by External Air Pressure," ASME Journal of Lubrication Technology, Vol. 96, pp. 247-249, 1974.
15. Dais, J.L., and Barnum, T.B., "The Geometrically Irregular Foil Bearing," ASME Journal of Lubrication Technology, Vol. 96, pp. 224-227, 1974.
16. Tanaka, K., "Analytical and Experimental Study of Tape Spacing for Magnetic Tape Unit - Effects of Tape Bending Rigidity, Gas Compressibility, and Molecular Mean Free Path," Tribology and Mechanics of Magnetic Storage Systems, ASLE Special Publication 19, pp. 72-79, 1985.
17. Heinrich, J.C., and Wadhwa, S.K., "Analysis of Self-Acting Foil Bearings: A Finite Element Approach," Tribology and Mechanics of Magnetic Storage Systems, Vol. III, editors, B. Bhushan, and N.J. Eiss Jr., pp. 152-159, 1986.

18. Rongen, P.M.J., "On Numerical Solution of the Instationary 2D Foil Bearing Problem," Tribology and Mechanics of Magnetic Storage Systems, ASLE Special Publication 26, pp. 130-138, 1989.

19. Heinrich, J.C., and Connolly, D., "Three-Dimensional Finite Element Analysis of Self-Acting Foil Bearing," Computer Methods in Applied Mechanics and Engineering, Vol. 100, pp. 31-43, 1992.

20. Eshel, A., and Wildmann, M., "Dynamic Behavior of a Foil in the Presence of a Lubricating Film," ASME Journal of Applied Mechanics, Vol. 35, pp. 242-247, 1968.

21. Eshel, A., "The Propagation of Disturbances in the Infinitely Wide Foil Bearing," ASME Journal of Lubrication Technology, Vol. 91, pp. 120-125, 1969.

22. Stahl, K.J., White, J.W., and Deckert, K.L., "Dynamic Response of Self-Acting Foil Bearings," IBM J. Res. Development, Vol. 18, pp. 513-520, 1974.

23. Granzow, G.D., "An Improved Foil Bearing Solution," M.S.Thesis, Department of Mechanical Engineering, University of New Mexico, 1980.

24. Granzow, G.D., and Lebeck, A.O., "An Improved One-Dimensional Foil Bearing Solution," Tribology and Mechanics of Magnetic Storage Systems, ASLE Special Publication *16*, pp. 54-58, 1984.

25. Tanaka, K., Oura, M., and Fujii, M., "Tape Spacing Characteristics of Cylindrical Heads With Taped Flat Surfaces for Use in Magnetic Tape Units," Tribology and Mechanics of Magnetic Storage Systems, Vol. III, editors, B.Bhushan, and N.J. Eiss Jr., pp. 130-137, 1986.

26. Yamauchi, T., Murakami, K., and Imamura, R., "The Air Permeability of Paper Related to the Porous Structure," Japan TAPPI Journal, Vol. 30, No. 5, pp. 273-280, 1976.

27. Brundertt, E., and Baines, W.D., "The Flow of Air Through Wet Paper," TAPPI Journal, Vol. 49, No. 3, pp. 97-101, March, 1966.

28. Riddiford, A.W., "Airflow Between a Paper and a Dryer Surface," TAPPI Journal, Vol. 52, No. 5, pp. 939-942, 1969.

29. Watanabe, Y., and Sueoka, Y., "Evaluation of Air Entrainment Between a Paper Web and a Roller," Presented at Technical Association of the Graphic Arts Conference, Kansas City, Mo., 1990.

30. Ducotey, K.S., and Good, J.K., "The Effect of Web Permeability and Side Leakage on the Air Film Height Between a Roller and Web," To appear in Journal of Tribology, 1997.

31. Kothari, S., "Computations of Air Films Between Moving Webs and Support Rollers," M.S. Thesis, School of Mechanical and Aerospace Engineering, Oklahoma State University, Stillwater, Oklahoma, May, 1996.

32. Lilley, D.G., Computational Fluid Dynamics, Vol. 1, Chapter 9, Lilley and Associates, Stillwater, Ok., 1992.

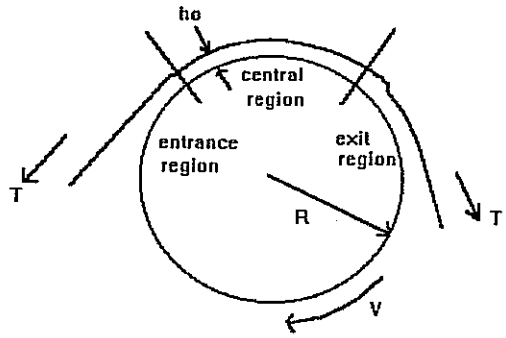

Figure 1. Schematic Diagram of a Foil Bearing

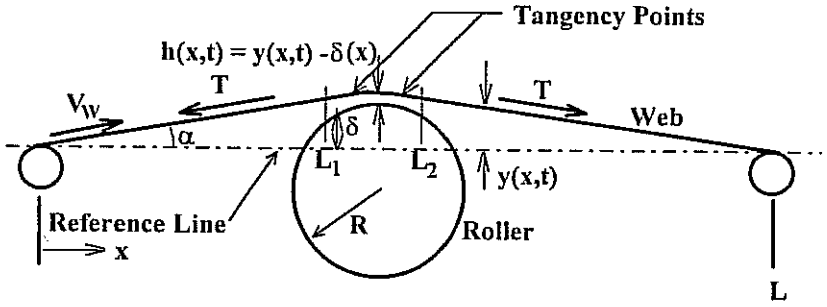

Figure 2. Schematic Diagram of Web-Roller Configuration Used in Computations

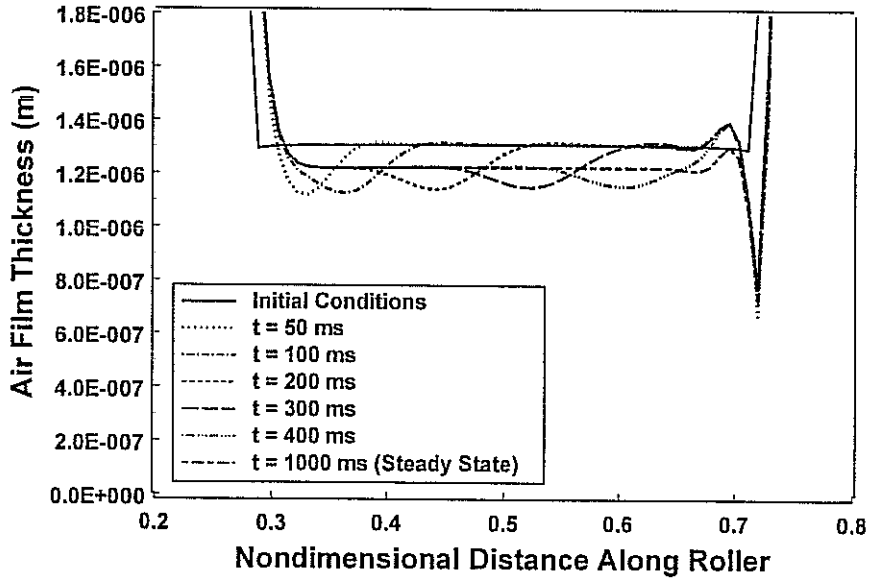

Figure 3. Transient Air Film Profiles for Moving Web and Stationary Support Cylinder

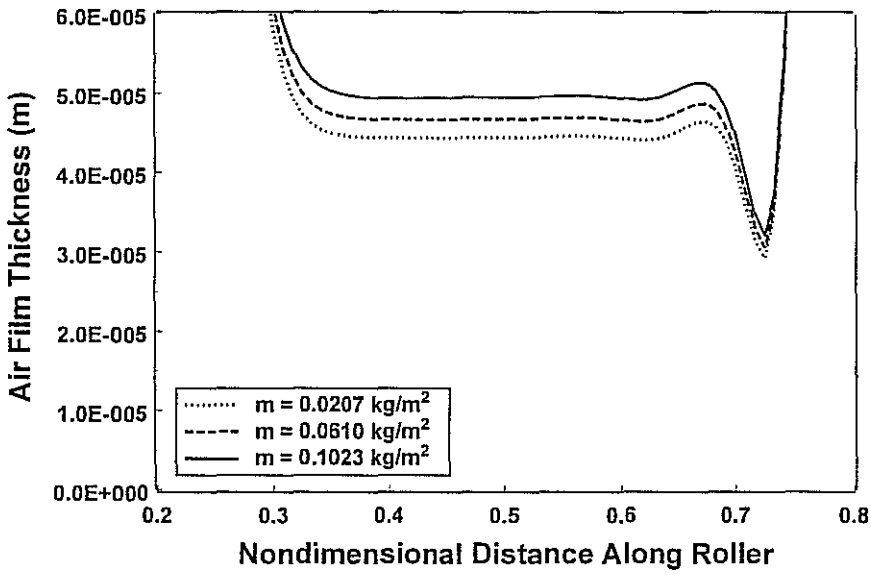

Figure 4. Effects of Web Mass on Air Film Profiles

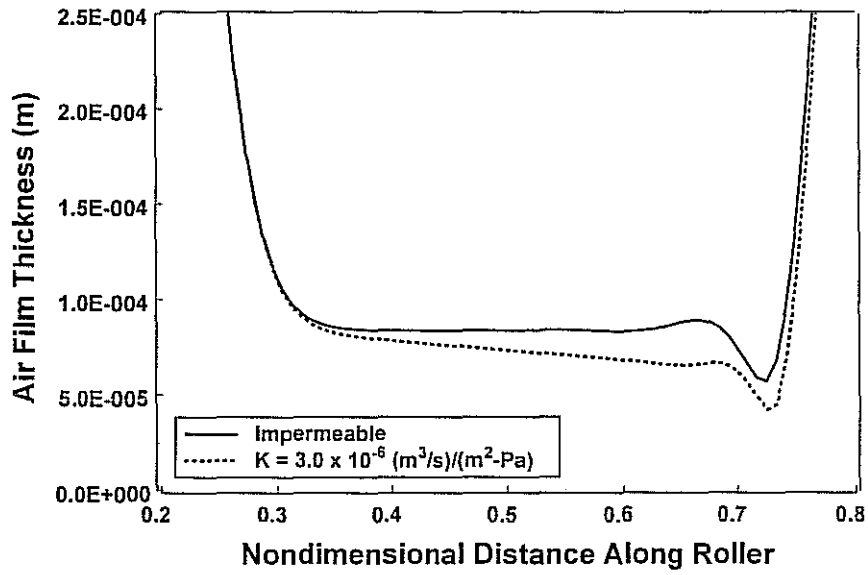

Figure 5. Effects of Web Permeability on Air Film Profiles

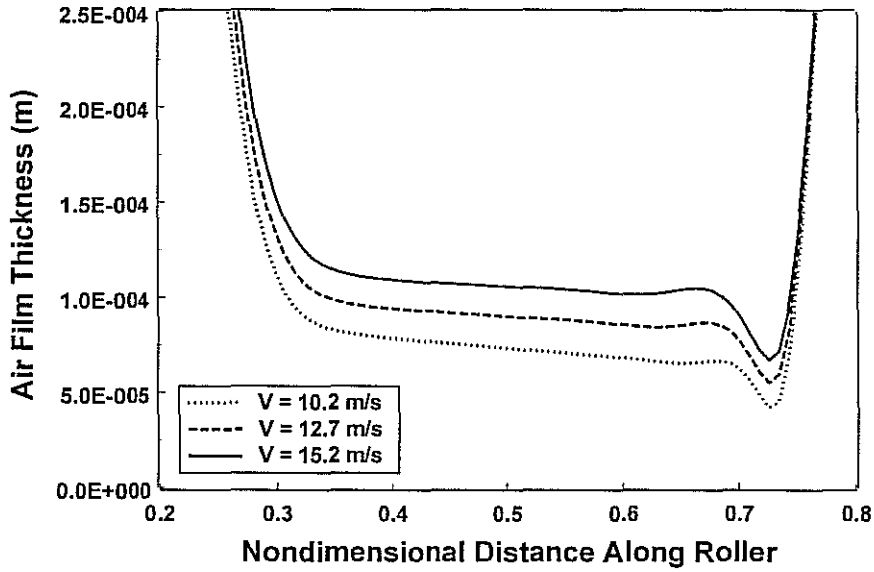

Figure 6. Effects of Web Permeability with Varying Velocity

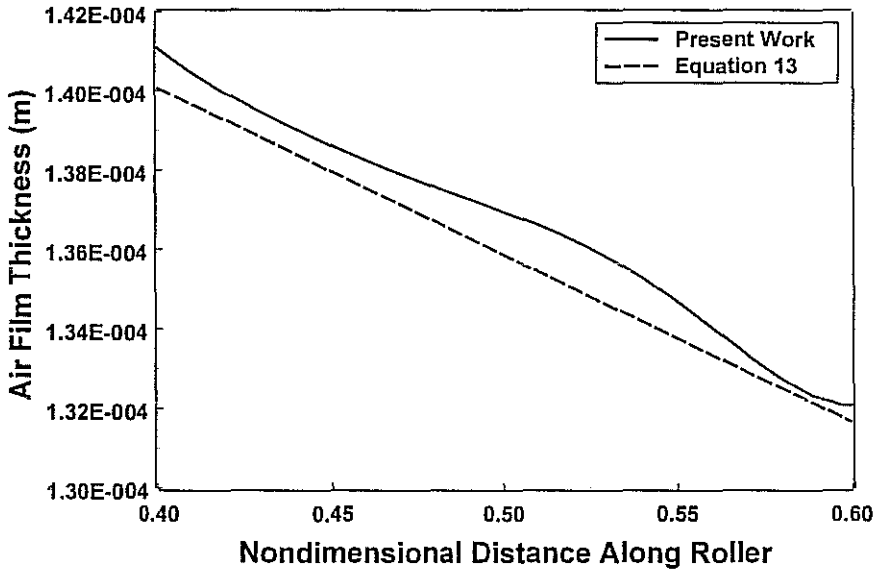

Figure 7. Comparison of Air Film Thickness Decreases in the Central Region for a Permeable Web

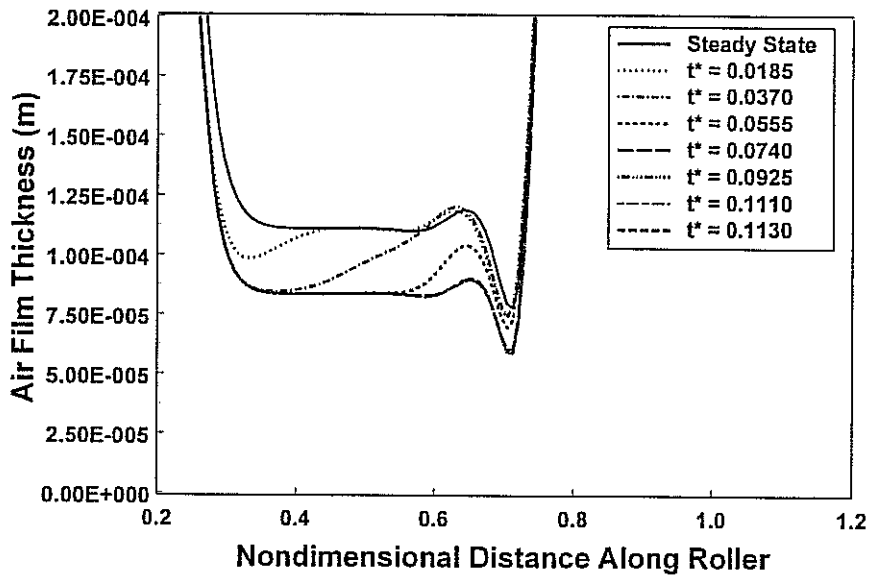

Figure 8. Transient Air Film Profiles for a 50% Step Increase in Tension for an Impermeable Web

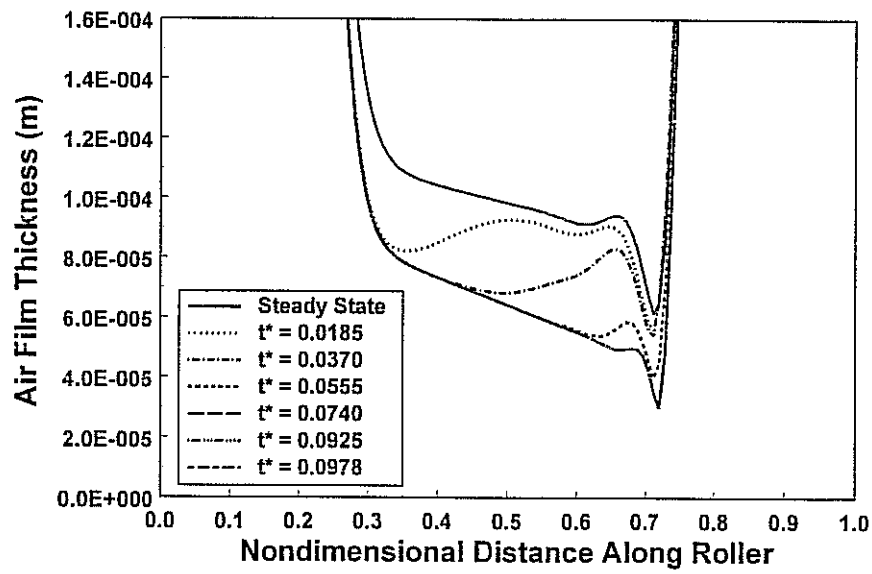

Figure 9. Transient Air Film Profiles for a 50% Step Increase in Tension for a Permeable Web

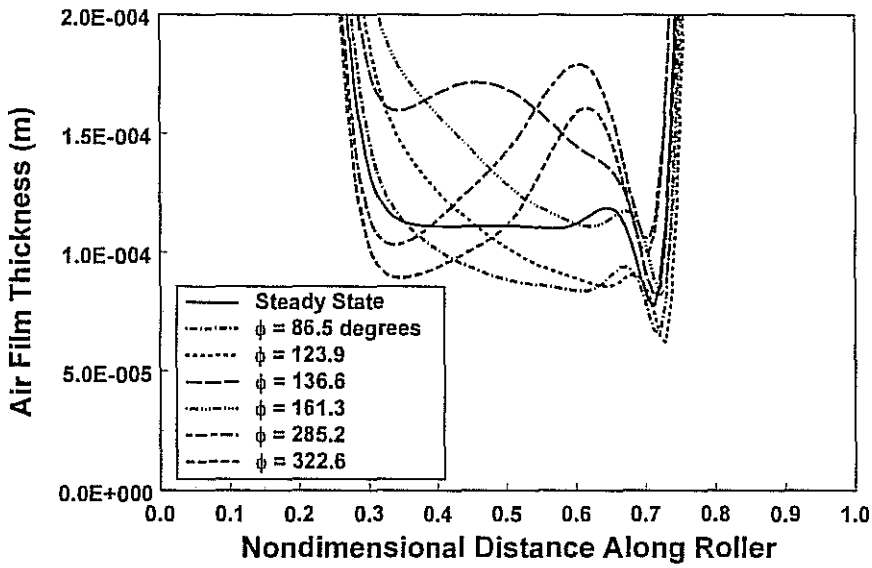

Figure 10. Transient Air Film Thickness Profiles for Sinusoidal Fluctuation in Tension for an Impermeable Web

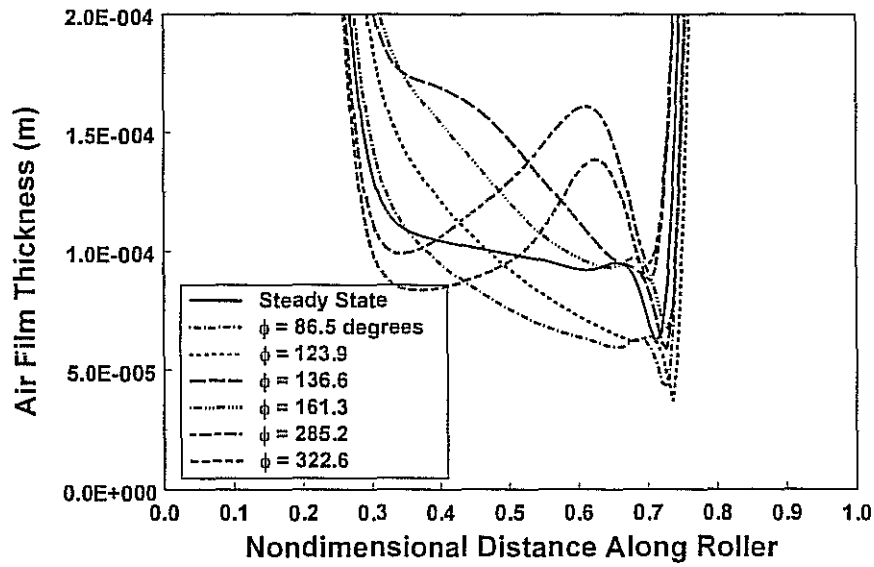

Figure 11. Transient Air Film Thickness Profiles for Sinusoidal Fluctuation in Tension for a Permeable Web

Question - In the transition case the flow conditions at the center are complicated. I'm not sure how to determine air 1 and air 2, and how to determine the air flow and the pressure condition? Please comment.

Answer - I'm not sure about reverse flow whether thats likely within the calculation or not the pressure there, I think that we are far enough away that it is atmospheric, we haven't verified these results otherwise I would show you, and for the dynamic case and I am also concerned about the clamped boundary conditions. I think the pressure is a good approximation at those points. Its something I can't answer very well, but it is something to take a look at.